E&G Quaternary Sci. J., 72, 77–94, 2023
https://doi.org/10.5194/egqsj-72-77-2023

Open Access E&G Quaternary Science Journal

Research article

Pleniglacial dynamics in an oceanic central European loess landscape

Stephan Pötter[1,2], Katharina Seeger[3], Christiane Richter[4], Dominik Brill[3], Mathias Knaak[5], Frank Lehmkuhl[1], and Philipp Schulte[1]

[1]Department of Geography, RWTH Aachen University, 52062 Aachen, Germany
[2]Chair of Geography, University of Koblenz-Landau, 56070 Koblenz, Germany
[3]Institute of Geography, University of Cologne, 50923 Cologne, Germany
[4]Institute of Geography, Technical University Dresden, 01069 Dresden, Germany
[5]Division Applied Geosciences, Geological Survey of North Rhine-Westphalia, 47803 Krefeld, Germany

Correspondence: Stephan Pötter (stephan.poetter@geo.rwth-aachen.de)

Relevant dates: Received: 13 May 2022 – Revised: 21 December 2022 – Accepted: 23 February 2023 – Published: 24 April 2023

How to cite: Pötter, S., Seeger, K., Richter, C., Brill, D., Knaak, M., Lehmkuhl, F., and Schulte, P.: Pleniglacial dynamics in an oceanic central European loess landscape, E&G Quaternary Sci. J., 72, 77–94, https://doi.org/10.5194/egqsj-72-77-2023, 2023.

Abstract: Loess–palaeosol sequences (LPSs) of the oceanic-influenced European loess belt underwent frequent post-depositional processes induced by surface runoff or periglacial processes. The interpretation of such atypical LPSs is not straightforward, and they cannot be easily used for regional to continental correlations. Within the last few years, however, such sequences gained increased attention, as they are valuable archives for regional landscape dynamics. In this study, the Siersdorf LPS was analysed using a multi-proxy approach using sedimentological, geochemical, and spectrophotometric methods combined with luminescence dating and tentative malacological tests to unravel Pleniglacial dynamics of the Lower Rhine Embayment. A marshy wetland environment for the late Middle Pleniglacial to the early Upper Pleniglacial was shown by colour reflectance and grain size distribution. Age inversions from luminescence dating paired with geochemical and sedimentological data reveal long-lasting erosional processes during the early Upper Pleniglacial, which were constrained to a relatively small catchment with short transport ranges. The upper sequence shows typical marker horizons for the study area and indicate harsh, cold-arid conditions for the late Upper Pleniglacial. In comparison with other terrestrial archives, the Siersdorf LPS shows that the Lower Rhine Embayment was more diverse than previously assumed, regarding not only its geomorphological settings and related processes but also its ecosystems and environments.

Kurzfassung: Die Lössprofile des ozeanisch beeinflussten europäischen Lössgürtels wurden häufig durch Oberflächenabfluss oder periglaziale Prozesse umgelagert. Die Interpretation solcher atypischen LPS ist nicht einfach und sie können nicht ohne weiteres für regionale bis kontinentale Korrelationen verwendet werden. In den letzten Jahren haben solche Sequenzen jedoch zunehmend an Bedeutung gewonnen, da sie wertvolle Archive für die regionale Landschaftsdynamik darstellen. In dieser Studie wurde das Lössprofil Siersdorf mit Hilfe eines Multi-Proxy-Ansatzes analysiert, der sedimentologische, geochemische und spektrophotometrische Methoden mit Lumineszenzdatierungen und ver-

suchsweisen malakologischen Untersuchungen kombiniert, um die pleniglaziale Dynamik der Niederrheinischen Bucht zu entschlüsseln. Die Farbadaten und die Korngrößenverteilungen zeigen, dass das Profil vom späten Mittelpleniglazial bis zum frühen Oberpleniglazial in einem sumpfigen Feuchtgebiet lag. Altersinversionen aus Lumineszenzdatierungen gepaart mit geochemischen und sedimentologischen Daten lassen auf lang anhaltende Erosionsprozesse während des frühen Oberen Pleniglazials schließen, die auf ein relativ kleines Einzugsgebiet mit kurzen Transportstrecken beschränkt waren. Die obere Abfolge zeigt typische Markerhorizonte für das Untersuchungsgebiet und weist auf raue, kalt-trockene Bedingungen für das späte Obere Pleniglazial hin. Im Vergleich zu anderen terrestrischen Archiven zeigt das Siersdorfer LPS, dass die Niederrheinische Bucht vielfältiger war als bisher angenommen, nicht nur in Bezug auf ihre geomorphologischen Gegebenheiten und die damit verbundenen Prozesse, sondern auch in Bezug auf ihre Ökosysteme und Lebensräume.

1 Introduction

Throughout the last few decades, loess–palaeosol sequences (LPSs) have been frequently analysed to reconstruct palaeoclimatic and palaeoenvironmental conditions of the terrestrial realms (Hatté et al., 2001, 2013; Marković et al., 2005; Kukla et al., 1988; Zech et al., 2013; Torre et al., 2020; Varga et al., 2011). Therefore, sequences are investigated, which are as complete and undisturbed as possible to allow interregional correlations (Marković et al., 2018; Lehmkuhl et al., 2016) or direct reconstructions of atmospheric conditions (Obreht et al., 2017; Rousseau and Hatté, 2021; Bokhorst et al., 2011). These aeolian LPSs were formed out of mineral dust, which was deposited on topographic barriers (Lehmkuhl et al., 2016; Antoine et al., 2016), biological crusts (Svirčev et al., 2013), or vegetation, typically grasses (Zech et al., 2013, 2011). The deposited dust undergoes quasi-pedogenic processes called loessification processes (Sprafke and Obreht, 2016), leading to its unique characteristics, such as its silty texture and porosity (Pécsi and Richter, 1996; Koch and Neumeister, 2005). Due to these properties, loess is prone to post-depositional reworking and erosion, especially by water (Meszner et al., 2013, p. 201), and in regions affected by permafrost, by periglacial activities and slope processes (Lehmkuhl et al., 2021, 2016). This proneness can lead to hiatuses in the stratigraphy (Obreht et al., 2015; Steup and Fuchs, 2017) or the reworking of sediments. Additionally, weathering and soil formation processes, such as decalcification, feldspar weathering, or lessivation of clay, can transform the pristine sediments on various scales and can give valuable hints on past environmental conditions (Fenn et al., 2020, 2021; Marković et al., 2018; Lehmkuhl et al., 2016).

The European loess belt (ELB; loess domain II sensu; Lehmkuhl et al., 2021), stretches from the shores of the English Channel (Antoine et al., 2003; Stevens et al., 2020) throughout Belgium (Haesaerts et al., 2016), Germany (Lehmkuhl et al., 2018), and Poland (Jary and Ciszek, 2013) towards Ukraine (Veres et al., 2018). Especially the western ELB (subdomain IIa sensu; Lehmkuhl et al., 2021), which is characterised by a humid, oceanic climate, was prone to erosional processes such as slope wash or solifluction (Lehmkuhl et al., 2016). These conditions led to frequent reorganisation processes of landscape systems due to widespread erosion throughout the ELB (Meszner et al., 2013), partially leading to relief reversals (Fischer et al., 2012; Kels, 2007; Lehmkuhl et al., 2015). The continental ice sheets to the north and the periglacially shaped central European uplands to the south dominated the Pleistocene palaeogeography of the ELB, acting as potential dust sources of Pleistocene loess deposits due to high production rates of detrital material (Baykal et al., 2021; Skurzyński et al., 2019, 2020; Vinnepand et al., 2022). Additionally, the climatic conditions and vicinity to continental and Alpine ice sheets induced periglacial conditions, especially during glacial and stadial phases (Jary, 2009; Lehmkuhl et al., 2021; Vandenberghe et al., 2014; Stadelmaier et al., 2021).

The results of these processes are, compared to other European loess regions like the Danube Basin (Marković et al., 2015), complex stratigraphic records with unconformities and polygenetic pedocomplexes in the western ELB. Therefore, complete Late Pleistocene LPSs, without any hiatuses or discordances, are scarce (Schirmer, 2002; Zens et al., 2018). Within the last few years, however, considerable attention was given to non-typical LPSs, which were either strongly reworked (Klinge et al., 2017; Steup and Fuchs, 2017; Meszner et al., 2014) or which were characterised by changing depositional milieus (Mayr et al., 2017; Sümegi et al., 2015; Hošek et al., 2017). These archives allow a detailed view of the interplay of climate, landscape development, and environment and are, therefore, a crucial addition to the vast set of Pleistocene sediment archives.

Here, we present geochronological and proxy data for a new LPS in the Lower Rhine Embayment (North Rhine-Westphalia, Germany). The Siersdorf (SID) LPS developed in a channel incised into an older Pleistocene terrace of the Meuse. It represents a high-resolution record of the transition from the late Middle (MPG) to the Upper Pleniglacial (UPG). Unlike typical LPSs from the area, the Middle Pleniglacial stadial conditions are not imprinted as a series of phases of

differently intense soil formation processes but as a uniform unit of greyish-brownish silt, most likely linked to semi-terrestrial marshy conditions. In this study, we analyse the sedimentological, geochemical, and spectrophotometric data to unravel the genesis of this atypical sedimentary succession. The geomorphological and palaeoenvironmental ramifications are discussed in the framework of loess research in the Rhine catchment. The Siersdorf LPS is a crucial addition to the framework of Pleniglacial landscape reconstruction, as it is so far the first reported LPS from the Lower Rhine Embayment which records semi-terrestrial conditions during the late Middle Pleniglacial to Upper Pleniglacial. This reconstruction shows that the Pleniglacial Lower Rhine Embayment was more diverse than previously assumed, regarding not only its geomorphological settings and related processes but also its ecosystems and environments.

2 Research area and study site

2.1 The Lower Rhine Embayment

The Lower Rhine Embayment (LRE) is part of the European rift system and covers the southernmost part of the Lower Rhine catchment. It is situated on the transition of the central European uplands, namely the Rhenish Massif, and the northern German lowlands (Böse et al., 2022). As a loess region, the LRE is part of the western European maritime (Atlantic) loess subdomain of the ELB sensu (Lehmkuhl et al., 2021). This part of the ELB was dominated by North Atlantic climate conditions during the Late Pleistocene (Antoine et al., 2001, 2009; Fischer et al., 2021). Due to the oceanic climate and the accompanied high landscape dynamics (Fischer et al., 2017), the distribution and characteristics of loess deposits in the LRE are strongly site-specific, depending on geomorphological settings and related processes.

Four main geomorphological positions for LPSs can be summarised (Lehmkuhl et al., 2016). LPSs in plateau situations are often affected by erosion, both by surface runoff and by deflation (Schirmer, 2016; Antoine et al., 2016). Additionally, chemical processes such as (carbonate) solution and leaching may affect these sequences. Slope positions in the LRE are especially prone to erosional processes. Truncation, e.g. related to phases of widespread erosion, may remove previously formed LPSs in their entirety (Schirmer, 2016). Similar conditions have been reported from adjacent regions of the ELB (Meszner et al., 2013; Antoine et al., 2016). Besides fluvial relocation, processes such as solifluction play a major role in slope positions (Lehmkuhl et al., 2016). Under periglacial conditions, a slope gradient of 2° is sufficient to initiate reworking by solifluction (Lehmkuhl, 2016). Relocated material is transported downslope and deposited on the slope toe. These positions act not only as sediment traps during loess formation (Antoine et al., 2016) but also as sinks of soil sediments and other relocated material (Kappler et al., 2018; Kühn et al., 2017). This also applies to depressions and erosional channels. Within these topographic sinks, detrital material of various origins, i.e. aeolian, colluvial, or other slope sediments, accumulates, leading to complex stratigraphical archives. As the geomorphological setting and sedimentological processes are crucial in the formation of sediment sequences, their discussion is essential to understand the evolution of LPSs and for their correlation with other environmental archives (Marković et al., 2018; Lehmkuhl et al., 2016; Fischer et al., 2017).

The LRE builds the easternmost part of this maritime loess domain, which shows comparable stratigraphic records for the Late Pleistocene from northern France towards the study area (Haesaerts et al., 2011; Meijs, 2002; Schirmer, 2016; Antoine et al., 2014): the oldest sequence builds the last interglacial, i.e. Eemian, palaeosol, a truncated brown-leached soil complex. The Weichselian glacial succession starts with an early glacial (115–72 ka) complex, consisting of a grey forest soil and a steppe-like soil. The Lower Pleniglacial (LPG; 70–58 ka) is the phase with the first reported (and preserved) loess formation in central Europe (Frechen et al., 2003), accompanied by periglacial conditions. The Middle Pleniglacial (MPG; 58–32 ka) was characterised by reduced dust accumulation (Antoine et al., 2001), frequent relocation of older sediments and soils (Meszner et al., 2013), and phases of soil formation (Fischer et al., 2021; Schirmer et al., 2012). However, MPG sequences are often only preserved in geomorphologically favourable settings. The Upper Pleniglacial (UPG; 32–15 ka) was characterised by enhanced dust accretion and harsh, periglacial conditions (Lehmkuhl et al., 2021). Typical features for these periods are Gelic Gleysols (tundra gleys) and ice-wedge casts (Antoine et al., 2016). In the LRE, the UPG deposits show a typical succession encompassing inter alia the so-called Eben Zone (Schirmer, 2003).

The study site is located within the so-called Aldenhoven loess plateau as part of the Börde region of Jülich (Knaak et al., 2021). This plateau, situated between the Wurm, Inde, and Rur rivers in the foreland of the northern Eifel Mountains (Fig. 1), is slightly inclined towards the northeast (170–75 m a.s.l.). Vast loess blankets cover the palaeorelief, which is characterised by small dendritic river systems. These blankets mainly formed during the Late Pleistocene as dust was entrained from the Middle Pleistocene terraces of the Rhine, Meuse, and Rur rivers. Steps in the landscape, where loess thicknesses vary considerably within a few metres, are indicative of recent differential tectonic processes. Late Pleistocene to Holocene features approx. 1 km northwest of the studied sequence, such as solifluction layers or other stratigraphic markers, show tectonically induced offsets of approx. 1 m, indicating younger tectonic movements (Fig. S1 in the Supplement). Additionally, tectonics shaped the hydrological system, as river deflections are abundant in the study area.

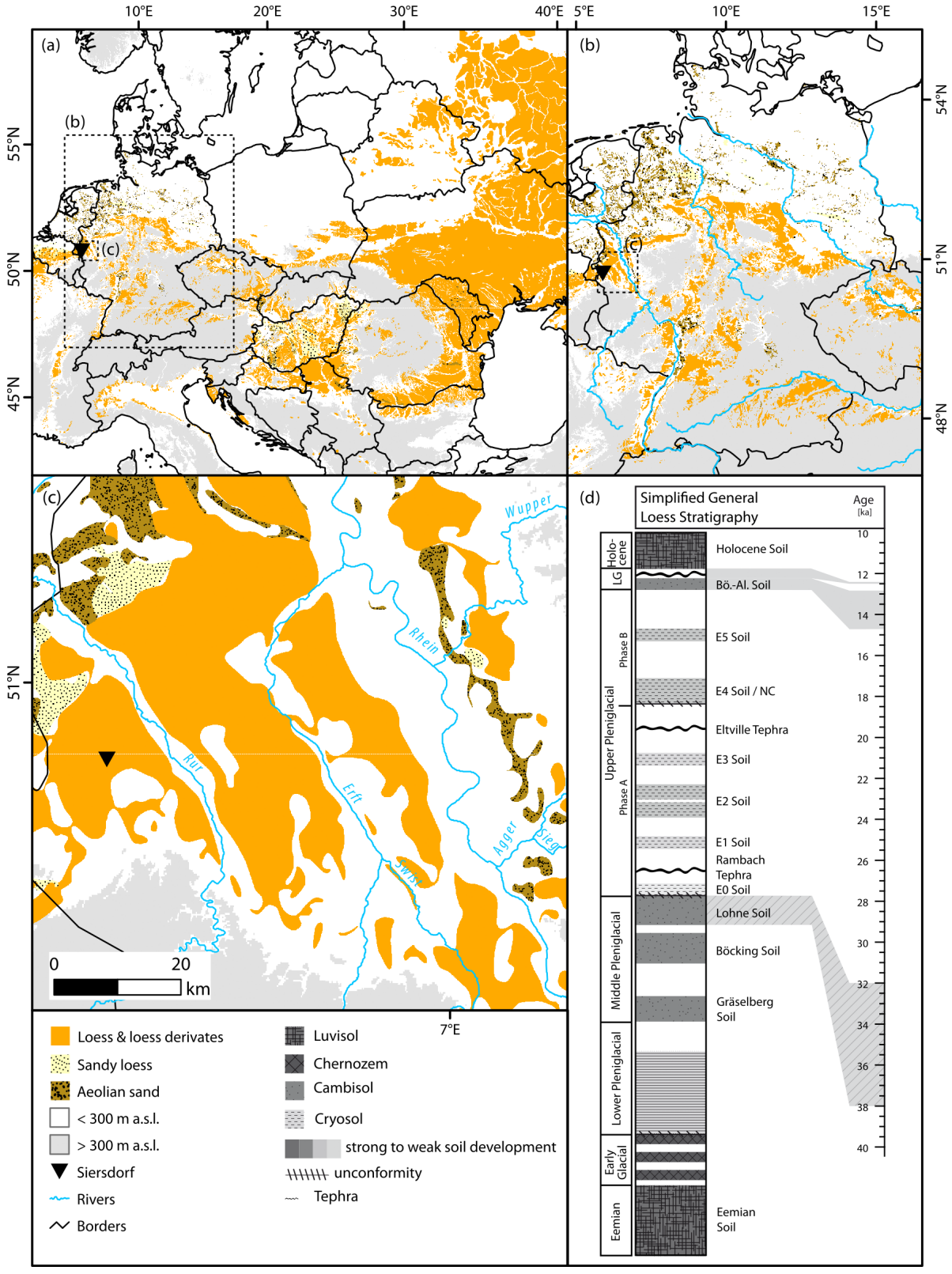

Figure 1. Location of the Siersdorf LPS (black triangle) **(a)** within the European loess belt, **(b)** in Germany, and **(c)** within the Lower Rhine Embayment. Distribution of aeolian sediment according to Lehmkuhl et al. (2021). **(d)** Simplified and generalised loess stratigraphy for central Europe, adapted from Zens et al. (2018).

2.2 The Siersdorf loess–palaeosol sequence

The Siersdorf (SID) LPS was exposed during construction works of the Zeelink natural gas pipeline in the central part of the Aldenhoven loess plateau (Fig. 1). The investigated sequence is 6 m thick (Fig. 2) and developed within a channel of a presumably Middle Pleistocene terrace of the Meuse. The deposits of the Meuse covered large parts of the central LRE during the Pleistocene (Boenigk and Frechen, 2006). The incised channel acted as a sediment trap throughout the Late Pleistocene and Holocene. Based on field observations, the sequence can be subdivided into five main units: the base, unit I, is characterised by greyish-dark-brownish silts, which change colour during drying to grey. Nearby core drillings indicate strong hydromorphic overprinting of these layers (Fig. S2). The upper part of this layer shows a high abundance of mollusc shells and shell fragments. The overlying loess (unit II) is laminated and partially characterised by cryoturbation features. At the base of this relocated loess, a thin, blackish layer occurs. The laminated layer stretches from 4.8 to 3.5 m below surface. Small ice-wedge pseudomorphs frequently disturb the layering, which shows varying contents of silt and sand. On top of the layered loess adjoins an orange, wavy layer (unit III). Greyish-brownish palaeosol layers, which show characteristics of Gelic Gleysols, built the uppermost part of unit III. Above this complex, the sequence consists of relatively unaltered loess (unit IV). This loess is also the fill material for massive ice-wedge pseudomorphs approx. 3 m left of the sampled section, which pierces the below-lying units until the top of the lowermost layer (Fig. 2). A humic, finely layered colluvial unit covers the loess (unit V). This reworked sediment contains small pebbles and charcoal flitters. The uppermost 90 cm of the sequence is anthropogenically disturbed.

3 Methods

3.1 Field work and sampling

The SID LPS was sampled in May 2021 after exposure during construction works of the Zeelink natural gas pipeline. Prior to description and sampling, several decimetres of exposed sediments were removed to avoid contamination with weathered and relocated material. The sequence was described in detail from the bottom to the top. Samples for sedimentological, geochemical, and colorimetric analyses were taken in a continuous sampling trench. Sampling was conducted using freshly cleaned tools and sterile plastic bags. The anthropogenically disturbed uppermost 90 cm was not sampled. The colluvial unit (0.9–1.7 m) was sampled in 10 cm increments, whereas the rest of the sequence was sampled every 5 cm.

For luminescence dating, six samples were taken horizontally with steel cylinders from selected units (for position of samples, see Fig. 2). Subsequently, the sediment within a 30 cm distance to the cylinders was sampled for dose rate determination.

3.2 Sedimentological, geochemical, and spectrophotometric analyses

The samples were dried at 35 °C, sieved to the fraction < 2 mm, and two subsamples of each sample (0.1 and 0.3 g) were pre-treated with 0.7 mL H_2O_2 (30 %) at 70 °C for 12 h. This process was repeated until bleaching of the material was visible (Allen and Thornley, 2004) but not longer than 3 d. To keep the particles dispersed during analysis, the samples were treated with 1.25 mL $Na_4P_2O_7 \cdot 10H_2O$ in an overhead shaker for 12 h. The grain size was determined with a Beckman Coulter LS 13 320 laser diffractometer using Mie theory (fluid refractive index (RI): 1.33, sample RI: 1.55, imaginary RI: 0.1) (Özer et al., 2010; Nottebaum et al., 2015; Schulte et al., 2016). Grain size distributions were calculated and visualised as distribution heatmaps according to Schulte and Lehmkuhl (2018, Fig. 3). To detect (neo-)formations of clay minerals, the differences between the two optical models of Mie theory and the Fraunhofer approximation were calculated and centred log transformed (Schulte and Lehmkuhl, 2018). The results are visualised as heatmaps as well (Fig. 4).

Inorganic geochemistry was analysed using energy dispersive x-ray fluorescence (EDPXRF) using a SPECTRO XEPOS. This device detects 50 elements from sodium (Na) to uranium (U), excluding erbium and ytterbium. The samples were sieved to the silt fraction (< 63 µm) and dried at 105 °C for 12 h. A subsample of 8 g for each sample was mixed with 2 g FLUXANA CEREOX wax, homogenised in a shaker. The sample was pressed to a pellet with a pressure of 19.2 MPa for 120 s. The measurements were conducted by means of a pre-calibrated method. Each sample was measured in duplicate, and the pellets were rotated by 90° between measurements to avoid matrix effects. Conspicuous samples, where the difference of both measurements was striking, were measured again in duplicate to avoid analytical artefacts. Geochemical data are visualised as depth plots and in the form of the A–CN–K ternary diagram according to Nesbitt and Young (1984). The carbonate content was defined volumetrically using a SCHEIBLER apparatus (ISO 20693, 1995; Schaller, 2000).

Spectrophotometric analysis was conducted using a Konica Minolta CM-5 spectrophotometer, following previously published methodologies (Eckmeier and Gerlach, 2012; Vlaminck et al., 2016). This device uses the diffused reflected light from a standardised source (2° Standard Observer, Illuminant C) to obtain the colour spectra of the visible light (360 to 740 nm). The results were converted to the CIELAB colour space ($L^*a^*b^*$) using the SpectraMagic NX software (Konica Minolta). The dried and homogenised samples were measured in duplicate and averaged.

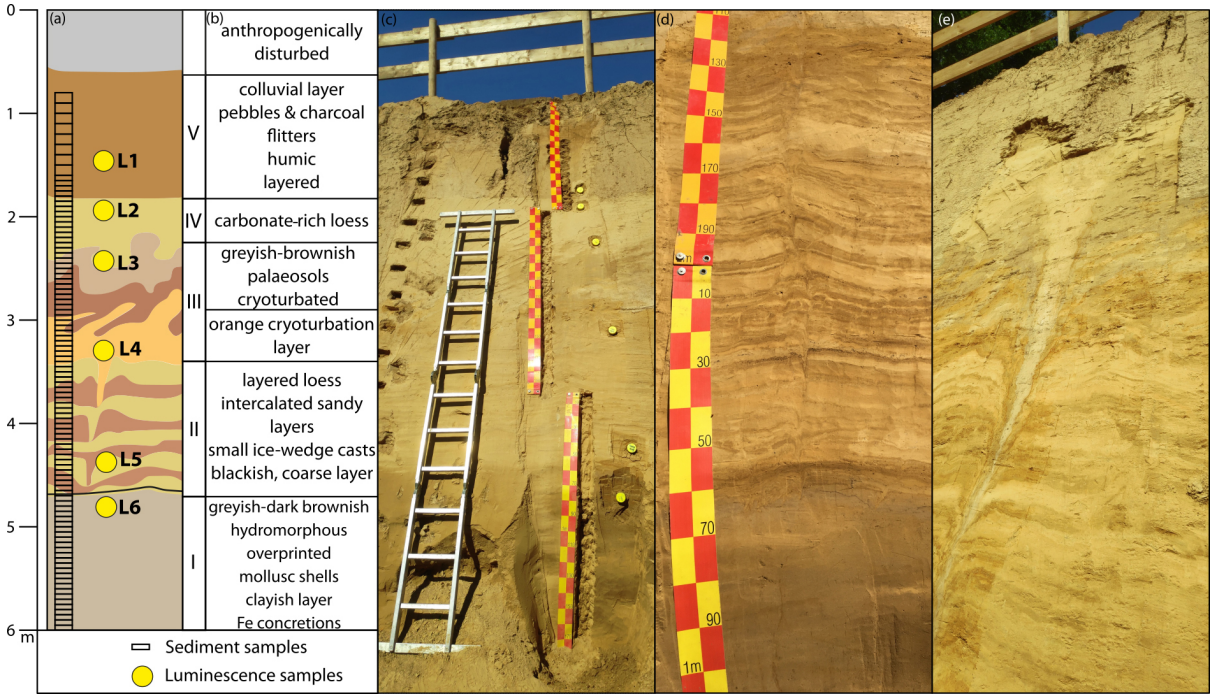

Figure 2. **(a)** Simplified stratigraphic sketch of the Siersdorf loess–palaeosol sequence. **(b)** Short description of main stratigraphic units. **(c)** Photo of the sequence after sampling (photo: Stephan Pötter). **(d)** Laminated loess package and basal palaeosol (photo: Philipp Schulte). **(e)** Ice-wedge cast, approx. 3 m left of the sampled sequence, piercing the underlying layers for more than 2 m (photo: Stephan Pötter).

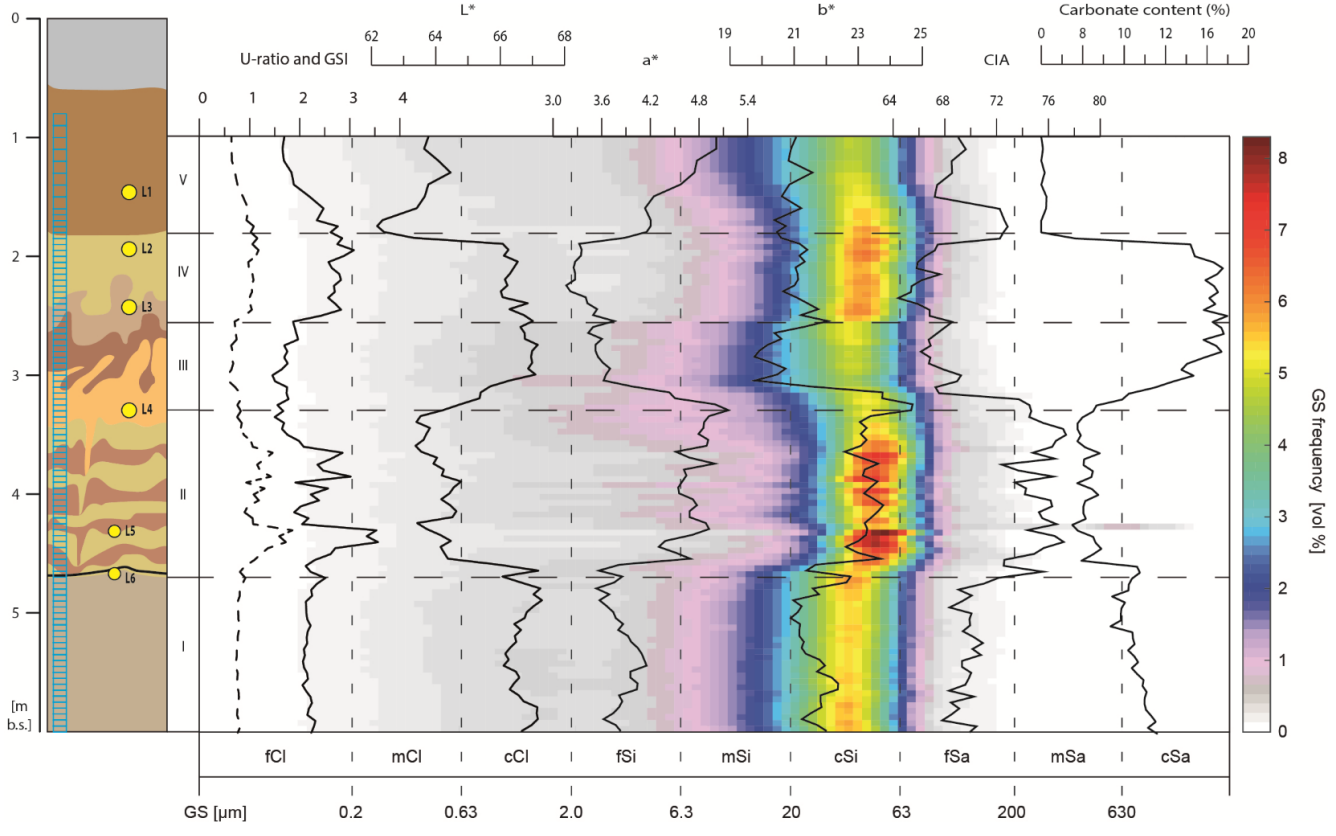

Figure 3. Heatmap visualisation of grain size distribution displayed with various sedimentological, geochemical, and spectrophotometric proxies of the Siersdorf LPS. Stratigraphic units (I–V) are shown for orientation.

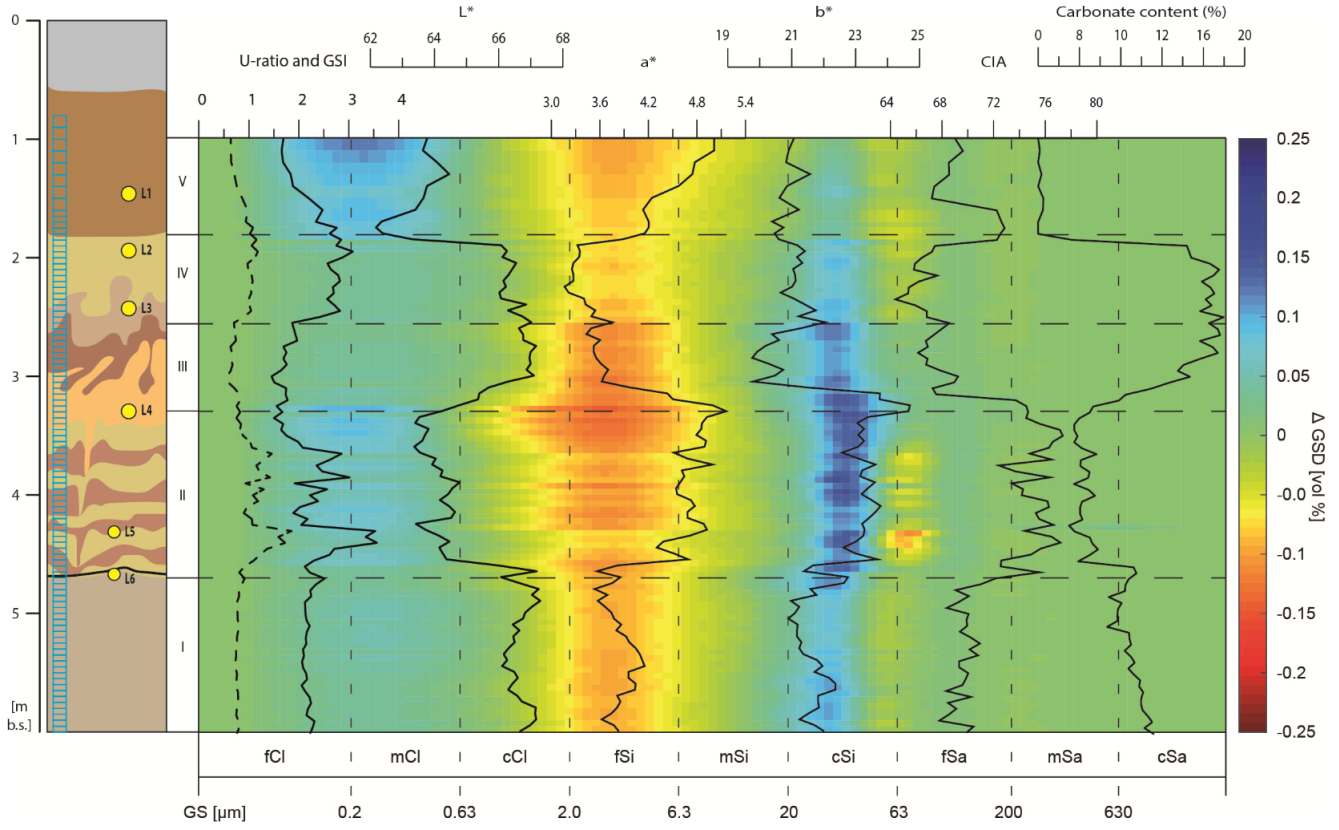

Figure 4. Heatmap visualisation of the difference between two optical models (ΔGSD) displayed with various sedimentological, geochemical, and spectrophotometric proxies of the Siersdorf LPS. Stratigraphic units (I–V) are shown for orientation.

3.3 Luminescence dating

Sample preparation and measurements were conducted in the Cologne Luminescence Laboratory (Cologne, Germany) and included pre-processing under red light conditions. Standard procedures of fine-grain preparation included chemical treatment with HCl (10 %), H_2O_2 (10 %), and $Na_2C_2O_4$ (0.01 N) to remove carbonates, organic components, and aggregates. The 4–11 µm fraction was then separated by settling due to gravitation and centrifugation following Frechen et al. (1996). To derive pure quartz, the 4–11 µm fraction was etched with HF (37 %) and finally washed with HCl (10 %).

Equivalent dose measurements were performed on an automated Risø TL/OSL DA-15 reader (DTU Nutech, Roskilde, Denmark) equipped with a calibrated $^{90}Sr/^{90}Y$ beta source. Discs were prepared by pipetting a suspension of 1 mg sediment and 0.2 mL deionised water and drying them afterwards. Polymineralic fine-grain samples were stimulated for 200 s by using infrared diodes (870 nm, FWHM = 40) and detected through an interference filter (410 nm). To obtain a feldspar signal not (or not significantly) affected by anomalous fading, a post-infrared infrared (pIRIR) stimulated luminescence protocol was applied with a second stimulation temperature of 290 °C ($pIRIR_{290}$) following Thiel et al. (2011). For quartz fine-grain samples, signals were stimulated with blue LEDs and detected through a U340 filter. Measurements followed a conventional single aliquot regenerative dose (SAR) protocol (Murray and Wintle, 2000).

The suitability of both measurement protocols for the samples of this study was tested based on preheat plateau (only for quartz samples) and dose recovery tests (for all samples). Furthermore, laboratory residual doses after solar simulator bleaching for 24 h and laboratory fading following Auclair et al. (2003) were determined for $pIRIR_{290}$ signals. For each sample, the palaeodose was calculated based on 5–12 accepted aliquots. Aliquots outside a 2σ range were excluded from further calculations. Since scatter in dose distributions of fine-grain samples is completely absent (reflected by overdispersions of around zero for all samples), the arithmetic mean plus standard deviation was chosen to calculate burial doses.

Dose rates were determined by measuring uranium, thorium, and potassium contents using high-resolution gamma spectrometry (Ortec PROFILE M-Series GEM P-type Coaxial HPGe Gamma-Ray Detector). Dosimetry and age calculation were conducted in the DRAC environment (version 1.2; Durcan et al., 2015) using typical water contents of European loess (i.e. 15 ± 5 %; Pécsi, 1990; Klasen et al., 2015) instead

of in situ measured ones, as these likely underestimate the hydromorphic conditions at the SID site. Further details on the measurement procedure of dose rate and equivalent dose determination are given in the Supplement.

4 Results

4.1 Sedimentological, geochemical, and spectrophotometric analyses

The grain size distributions (GSDs) of SID show typical patterns for central European loess deposits. Figure S3 shows the distribution curves for all main units identified during fieldwork. The lowermost unit I shows a unimodal GSD with a mode in the middle-coarse silt fraction. The contents of fine particles, especially fine silt and clay, are elevated. The laminated loess unit shows high variations in GSDs. The overlying cryoturbated loess layers show less variations, with strong modes in coarse silt and varying clay and sand contents. The GSD of the brownish-greyish palaeosol also shows a unimodal shape with a mode in coarse silt. Since other fractions, especially clay, are increased, this mode does not show as high values as the other layers. The uppermost loess layer shows a strong coarse silt mode, whereas the colluvial unit is relatively clay rich.

The geochemical results (Figs. 3–5) were utilised to calculate the Chemical Index of Alteration (CIA; Nesbitt and Young, 1982) to determine phases of enhanced chemical weathering. The basal complex does not show any variations in the CIA with all values being lower than 70. The laminated loess package shows higher values of > 70, as does the orange cryoturbated layer. The uppermost loess layer again shows decreased values, with a peak on the base of the overlying colluvial unit. The A–CN–K ternary diagram shows a distribution broadly parallel to the CN join, which can be broadly divided into two clusters (Fig. 5). The lower cluster is uniformly parallel, whereas the upper cluster shows some tendencies towards a more vertical distribution. A similar pattern is reflected by spectrophotometric analyses. The lower unit shows slight variations in the L^*, a^*, and b^* values. The layered unit shows rapidly decreased L^* and increased a^* and b^* values. The orange cryoturbated layer shows the maximum values for a^* and b^*, whereas the upper loess shows decreased redness and yellowness values. The colluvial unit is characterised by dark (low L^*) and brown colours (high a^*).

4.2 Luminescence dating

The results of the luminescence experiments are presented in the Supplement. All parameters relevant for age calculation and calculated ages for the six luminescence samples are presented in Table 1. Palaeodoses were calculated based on De measurements of 5–10 aliquots that were all accepted for data analysis (the very low scatter between De values did not require a larger number of aliquots). Given the absence of significant over-dispersion (Figs. S11 and S12), the arithmetic mean was chosen as the appropriate age model.

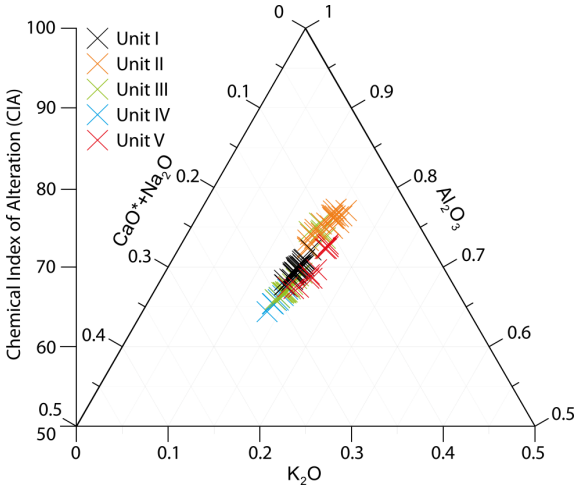

Figure 5. A–CN–K ternary diagram according to Nesbitt and Young (1984) for the Siersdorf LPS. The Chemical Index of Alteration is displayed on the y axis.

For polymineralic samples, burial doses range from 77 ± 1 Gyr (SID L1) to 177 ± 5 Gyr (SID L4). For the uppermost five samples, resulting ages are in stratigraphic order (Fig. 6). In contrast, the quartz ages are in line with the whole sedimentary sequence except for SID L1. Here, the quartz age of 34 ka significantly overestimates the feldspar age of 16 ka. Since it causes an inversion compared to the layers dated below, the quartz age of SID L1 should not be trusted. We have no explanation for this overestimation (since the pIRIR ages are significantly younger, this cannot be a bleaching issue), but this unit must be younger than at least 20 ka (SID L2). For SID L2 and L3, both quartz and feldspar ages are identical and yield ages of 18 to 23 ka. The quartz and $pIRIR_{290}$ ages calculated for samples SID L4 and L5 overlap within their uncertainties. The quartz and $pIRIR_{290}$ ages for SID L6 show an age inversion to the samples above and are therefore not stratigraphically consistent.

5 Discussion

5.1 Formation processes of an atypical loess sequence in the Lower Rhine Embayment

The Siersdorf LPS is a valuable archive for Weichselian Pleniglacial landscape dynamics. Combined sedimentological, geochemical, and spectrophotometric methods reveal distinct changes of environmental conditions and associated geomorphic processes during the formation of the investigated LPS, indicating a more heterogeneous environment in the LRE than previously assumed.

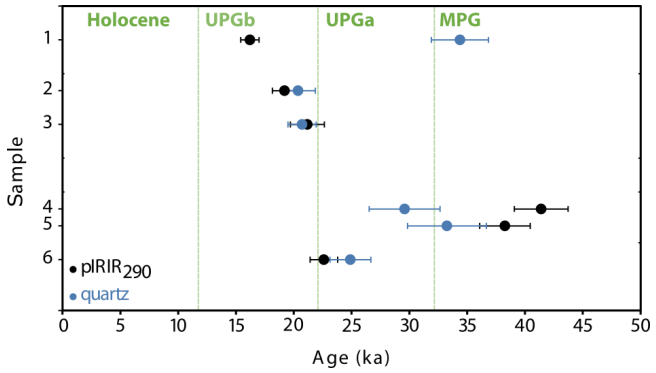

Figure 6. Age depth plot with feldspar ages and quartz ages. Age estimates for the Middle Pleniglacial (MPG), early Upper Pleniglacial (UPGa), late Upper Pleniglacial (UPGb), and the Holocene according to Zens et al. (2018).

5.1.1 Unit I

Unit I shows uniform patterns in most of the analysed proxy data. Especially the GSD and ΔGSD show almost no variations within this unit (Figs. 3 and 4). The low, uniform ΔGSD excludes this unit as a palaeosol, as pedogenic processes would favour the formation of clay minerals (Schulte and Lehmkuhl, 2018), which was observed for LPSs in the Rhine–Meuse catchment (Zens et al., 2018). The lack of large quantities of sand, as well as the uniform GSD of the unit, excludes large-scale relocation processes, pointing to an in situ formation of this unit. In-field measurements of the magnetic susceptibility in SID revealed low values for the respective lithological unit (Knaak et al., 2021), precluding biogenic formation of iron oxides. The proxy data, e.g. the low and uniform ΔGSD, indicate that unit I does not represent a typical interstadial palaeosol.

The unit's bright-greyish hues, shown by high L^* and low a^* and b^* values (Fig. 3), indicate a reductive milieu during or after deposition of the medium-coarse silt. The uniform sedimentology together with these grey shades point to a depositional milieu differing from the typical dust traps such as topographic barriers (Antoine et al., 2016; Lehmkuhl et al., 2016) or vegetation. A possible explanation for these prevailing reductive conditions would be a dust deposition in a semi-terrestrial environment. Such an environment was reported from the Bobingen LPS (BOB) in southern Germany (Mayr et al., 2017). The site was covered by a lake during the MPG, which is reflected by highly reduced blueish-greyish sediments and lacustrine faunal remains. During the late MPG, the lake silted up, and typical subaerial loess formation began. A similar situation was reported from the Ringen LPS (RGE) in the Middle Rhine Valley, where a gyttja was correlated to the MPG based on palynological evidence (Henze, 1998). This unit shows blueish-greyish hues and a silty-clayey texture and is approx. 2 m thick (Fig. S4). The colour and texture change towards the top, as the top is more oxidised and contains coarser grains. This succession reveals that the gyttja at the Ringen LPS, as a trap for both moisture and mineral dust, was continually covered by increased input of aeolian detrital material during the MPG–UPG transition, silting up the marshy environment. Similar conditions have been reported from the Bína LPS in Slovakia, although these were correlated to the Lower Pleniglacial (marine isotope stage (MIS) 4) (Hošek et al., 2017).

Besides macroscopic similarities between the two units of SID and RGE, the respective sedimentological evidence also points to similar environmental conditions. Both LPSs show unimodal GSDs, dominated by medium-coarse silt with slightly elevated clay contents (Fig. S3). These distributions indicate input of aeolian dust. Increased sand contents indicate additional but considerably less input by surface runoff. The water-saturated conditions are imprinted not only in greyish colours and sedimentology but also in wavy, flaky structures reported from field observations, indicating a micro-layering in a quiescent depositional environment. In RGE and BOB, the sediment is completely bleached and shows signs of intense reduction of ferruginous compounds, namely blueish-greyish hues. In SID, however, the lower intensity of reduction processes indicates shorter phases of semi-terrestrial conditions compared to the former sites. However, another plausible explanation is that the unit did not develop under proper lacustrine conditions comparable to BOB or RGE but in a marshy wetland situation, presumably with seasonal drying phenomena.

Within around 10 %, the carbonate content within unit I allowed the preservation of a high number of mollusc shells and shell fragments. Although no samples according to proper malacological protocols were taken, some cautious interpretation of malacofauna is feasible, always against the backdrop of the methodological issues. For this rough screening, bulk sediment samples from unit I were wet sieved (2 mm mesh) to separate the molluscs from the sediment. The tentative analyses show a poor species community with only two species comprising a high number (> 2000 individuals) of *Trochulus hispidus* and a smaller number (< 30 individuals) of *Succinella oblonga*. Both are euryoecious species, tolerating a wide range of conditions. The high number of shells that stood out visually in this layer is an indication that there was more vegetation and thus food supply and shelter compared to the rest of the sequence. However, *Trochulus hispidus* as well as *Succinella oblonga* are typical representatives of the poor snail communities found under extreme environmental conditions within Pleistocene loess ecosystems (e.g. Moine, 2008), as they are highly adaptable and able to tolerate both drought as well as temporary flooding. Their mere presence might indicate frequent wet-to-waterlogged ground conditions due to a depressed relief, permafrost-caused impermeable subsoil, and enhanced precipitation. Although caution is required due to methodological deficits, the low biodiversity and imbalance in the distribution of individuals among species equally indicate a highly

stressed ecosystem and harsh conditions. Better conditions e.g. due to better-drained grounds and longer vegetation periods usually relate to a higher biodiversity within the snail communities (see Moine, 2008). For a more reliable interpretation, however, a detailed examination of the gastropod fauna is necessary, including an adequate sampling technique and analyses of the complete sequence.

From a geomorphogenetic point of view, the position of SID in an incised channel favours both sediment accumulation and moisture availability (Lehmkuhl et al., 2016). Especially during times with waterlogging, e.g. induced by permafrost conditions, moisture became concentrated in such depressions. These conditions led to the formation of wetlands, with temporary flooding within the channel caused by increased precipitation. As the Late Pleistocene was characterised by several phases of relatively enhanced dust fluxes (Zens et al., 2018; Fischer et al., 2021), and the SID site is located near potential dust sources, mainly the Pleistocene braided systems of the Meuse and the Rhine, as well as their tributaries (Lehmkuhl et al., 2018), these ponds were subjected to periodical inputs of aeolian dust. Although unit I partially shows slightly elevated sand contents (Fig. 3), the generally fine and particular unimodal GSD indicates input of aeolian dust into this marshy environment as the major sedimentological process.

5.1.2 Unit II

After the marshy environment was covered with aeolian dust, formation of unit II began. This unit's main characteristics are a distinct layering with alternating dark brown and ochre-beige bands as well as small ice-wedge pseudomorphs permeating the layers. Generally, the transition from unit I to unit II shows sharp decreases or increases in most analysed proxies (Figs. 3 and 4). Especially the GSD from a medium-coarse silt mode to a mode bordering the fine-sand fraction may indicate erosional processes during this transitional period. Layered units in LPSs are well known from the ELB (Lehmkuhl et al., 2021; Antoine et al., 2016, 2001, 2013). They are usually correlated to the Upper Pleniglacial Hesbaye loess (Haesaerts et al., 2016; Schirmer, 2016) and are explained by a shift towards colder, more humid climatic conditions, including extensive snow covers during winter. Dust sedimentation on snow covers leads to a fine lamination, which is most likely due to micro-sorting processes during snowmelt. These laminations are usually a few millimetres thick with sandy bases fining-up upwards (Antoine et al., 2001). The laminations in SID, however, are partly several centimetres thick and show distinct differences in both colour and grain size. These differences show up by the reflectance data and the grain size patterns: generally, unit II is coarser than unit I. Additionally, it shows larger GSD variations with sandier bands. These sandier bands usually show higher a^* values and a higher CIA, indicating soil sediment eroded from higher topographic positions deposited in the channel. The GSD, especially with the high fluctuations of sand contents, excludes in situ soil-forming processes in this unit, although the ΔGSD is elevated in the clay fraction compared to unit I. Usually, this proxy is an indicator for in situ soil formation, as it reflects the neo-formation of clay minerals (Schulte and Lehmkuhl, 2018). In the case of unit II, however, the high ΔGSD together with other granulometric and sedimentological features rather point to a short-range transport of eroded soil material, where clay agglomerates were not destroyed during transport, and clay particles were not removed by further outwash. The stratigraphic inconsistencies of the luminescence ages (see Fig. 6 and Sect. 4.2) also indicate relocation by surface runoff, hindering complete bleaching of the material. Relatively low contents of carbonate within unit II also point to soil sediments, as carbonates were removed by leaching prior relocation. The lighter bands are associated with higher grain size index (GSI) and U-ratio values due to increased aeolian input of mineral dust or rather increased deposition of relocated loess (Fig. 4). The slightly vertical point distribution within the upper cluster of the A–CN–K ternary diagram, a feature which indicates hydraulic sorting (Pötter et al., 2021; Ohta, 2004), also points to reworking. Unit II was frequently overprinted by harsh, periglacial conditions, as indicated by a multitude of small, centimetre-scale ice-wedge casts permeating several layers of the package. The sedimentological features of the unit are the results of fluctuating environmental conditions during the formation phase of unit II.

5.1.3 Unit III

Unit III of the SID LPS shows a characteristic succession of an orange layer and two distinct palaeosol layers (Fig. 2). The sediments of unit III generally have finer GSD modes compared to unit II, paired with a slightly decreased U ratio and GSI. The entire unit shows evidence of heavy reworking by cryoturbation, especially wavy-layer contacts and low ΔGSD values for the clay fraction. This succession strongly resembles the so-called Eben Zone (see Sect. 5.2), which is an important UPG marker horizon for the oceanic ELB (Lehmkuhl et al., 2021; Schirmer, 2003). This zone is reflected in the proxy data, e.g. by enhanced clay contents and low GSI and U-ratio values between 3 and 2.5 m depth. The reworking of the soil material is expressed in the absence of very fine particles, shown in the ΔGSD ratios (Fig. 4). Generally, unit III shows fewer signs of intensive soil formation processes and less evidence for reworking by surface runoff than the layers of unit II. The carbonate contents and L^* values are increased as opposed to the decreased CIA and a^* values (Fig. 3).

5.1.4 Unit IV

Unit IV is composed of relatively unaltered loess. The unit is well sorted and is characterised by a typical GSD for cen-

tral European loess deposits, showing a strong mode in the coarse silt fraction (Fig. S3). The high carbonate contents of approx. 20 % and L^* values of approx. 66 show characteristic values for pristine Late Pleistocene deposits of the western ELB. Unit IV was, therefore, formed by the deposition of aeolian dust and subsequent loessification processes. The sharp contact to the above-lying unit V, however, both observed in the field and in proxy data (Figs. 3 and 4), points to a phase of erosion after unit IV was formed.

5.1.5 Unit V

The uppermost unit V shows a combination of no carbonate, high a^* values, and reflectance (L^*). Macroscopic features, such as the fine layering and the high abundance of charcoal flitters, together with lack of carbonate and relatively uniform GSD, point to a colluvial origin of this layer. During colluviation, (soil) sediment eroded from higher positions was transported to and deposited at the site. Additionally, the layer was influenced by post-depositional alterations, such as decalcification.

5.2 Reconstruction of Pleniglacial dynamics

In combination with the luminescence dating results (see Sect. 3.2), the formation processes of the Siersdorf LPS draw a detailed picture of regional imprints of the late MPG–UPG transition in the western ELB. The Pleniglacial dynamics of the SID site are summarised in the following conceptual model (see also Fig. 7). The correlation of unit I to the MPG–UPG transition (Fig. 7a and b) is based on one sample (SID L6) near the upper boundary of the unit. Luminescence analyses yield ages of 24.9 ± 1.8 ka (Q) and 22.6 ± 1.2 ka (KF, potassium feldspar) respectively. These ages indicate that the marshy environment at SID prevailed at least until the Upper Pleniglacial phase a (UPGa) sensu (Zens et al., 2018). Nearby core drillings, however, show that this unit is in total approx. 2 m thick, reaching a depth of around 7 m (Fig. S2). Therefore, the waterlogged environment in the incised terrace channel occurred during large parts of the UPGa and most likely also during the MPG–UPG transition. This interpretation, however, is based on the SID L6 sample and stratigraphic evidence. Further and more detailed reconstructions of fluctuations within the MPG require a denser chronological framework, e.g. by radiocarbon dating of mollusc shells. Nonetheless, the here-presented data allow a tentative correlation of unit I to the MPG–UPG transition.

The MPG, closely correlated with the MIS 3, was a phase of severe environmental fluctuations in the ELB. Periods of climatic ameliorations and pedogenesis, due to higher moisture availability (Fischer et al., 2021; Antoine et al., 2013; Schirmer et al., 2012; Hošek et al., 2017; Vinnepand et al., 2020), alternated with periods of erosion and (re-)deposition of soils and sediment (Meszner et al., 2011, 2013). Phases of soil formations can be traced in proxy data, as the ΔGSD signals (Zens et al., 2018), organic carbon contents (Fischer et al., 2021), or the a^* values increase in palaeosols (Krauß et al., 2016), whereas relocation can be reconstructed e.g. using grain size data (Meszner et al., 2014). In SID, the late MPG and early UPG are characterised by marshy conditions (see Sect. 5.1). These conditions were favoured by waterlogging

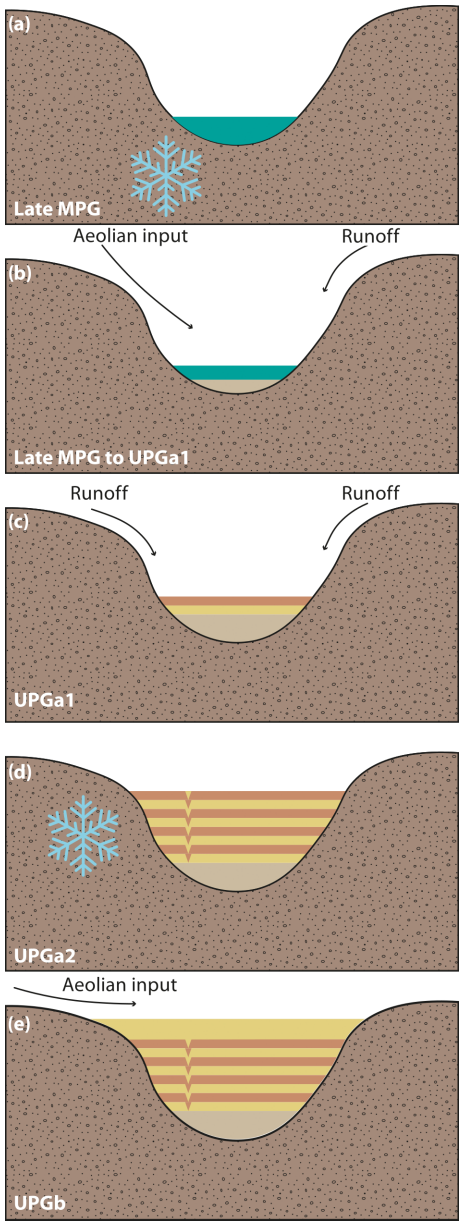

Figure 7. Schematic model of the Middle and early Upper Pleniglacial site formation of the Siersdorf LPS. **(a)** Marshy wetland conditions during the late MPG. **(b)** Silting up by aeolian input and surface runoff during the late MPG to early UPG. **(c)** Formation of layered unit by relocation of silty and sandy material by surface runoff in the early UPG ($UPGa_1$). **(d)** Periglacial overprinting and deformation of the layered unit during the LGM ($UPGa_2$). **(e)** Typical, subaerial loess formation during the UPGb.

due to permafrost (Fig. 7a), which was observed for other regions of the ELB (Sedov et al., 2016). These conditions are also reflected in the tentative malacological results, which show a potentially wet environment where the faunal assemblages were subjected to environmental stress.

The silting up of the marshy environment lasted during the MPG–UPG transitions until the early UPG (UPGa sensu; Zens et al., 2018). This phase of rapid climatic deterioration is in European loess landscapes coupled with a strong increase in dust production and subsequent loess formation (Meszner et al., 2013; Meyer-Heintze et al., 2018; Lehmkuhl et al., 2016; Antoine et al., 2013, 2009). This period is considered the phase with the highest dust accumulation rates in Europe (Zens et al., 2018; Frechen et al., 2003). In the LRE and other oceanic-influenced loess regions, the loess deposits of the beginning UPG, the so-called UPGa (Lehmkuhl et al., 2016; Zens et al., 2018, 2017), are named Hesbaye loess, (Schirmer, 2016) after the Belgian loess region (Haesaerts et al., 1997, 1981). The layered Hesbaye loess is often characterised by fluvial reworking or by dust deposition and loess formation under snow-influenced conditions. This feature is typical for the ELB and can be found from France towards the East European Plain (Antoine et al., 2009; Zens et al., 2018; Lehmkuhl et al., 2021). In SID, the layered unit II is dated by the quartz ages of samples SID L4 and L5 to 36.7–26.5 ka (Fig. 6). These calculated ages are stratigraphically inconsistent compared to SID L6, indicating deposition of older material after the formation of unit I. The inherited older ages of L4 and L5 as well as slightly older feldspar ages point to incomplete bleaching due to the relocation of the sediment, which points to a short transport range during sediment transport by surface runoff. The erosional processes during the MPG–UPG transition and the early UPG are widespread phenomena within the ELB (Meszner et al., 2013), often removing large parts or even entire MPG successions. The proxy data of unit II, in combination with the luminescence properties, allow for a reconstruction of short-scale transport of Middle Pleniglacial soil material during the UPGa, particularly to the steppe phase (Zens et al., 2018; Sirocko et al., 2016). The relocated material was frequently subjected to harsh, periglacial conditions, as indicated by a multitude of small ice-wedge casts (Fig. 2). Based on these geomorphological features, the periglacial overprinting is correlated to the tundra stage of the UPGa (Zens et al., 2018; Sirocko et al., 2016) where cold, dry conditions prevailed.

The later UPG succession (UPGb; Lehmkuhl et al., 2016; Zens et al., 2018, 2017) is also known as the Brabant member in the regional stratigraphy and mostly reflects loess formation during fully glacial conditions (Schirmer, 2016, 2000). Samples L4 and L3 bracket the orange and brownish-greyish complex of unit III, with ages between 30 and 21 ka. The ages, especially derived from quartz minerals (L4: 29.6 ± 3.1 ka; L3: 20.7 ± 1.2 ka), as well as the characteristics of this unit, allow a correlation with the so-called Eben Zone, composed of the orange Kesselt layer and the brownish-greyish Belmen and Elfgen soils (Schirmer, 2003). The high overlap of quartz- and feldspar-derived luminescence ages can be explained by the aeolian origin of this layer, which was indeed overprinted by periglacial processes but not by relocation. This characteristic zone is restricted to the Lower Rhine area and is a key marker layer for the UPG (Zens et al., 2018; Lehmkuhl et al., 2016, 2021). Samples L3 and L2 reflect the MIS 2 age of the Brabant loess. Their partial overlap within uncertainties allows a tentative, semi-quantitative reconstruction of accumulation rates, which were the highest during the LGM. This is in accordance with the general aeolian setting of the ELB (Rousseau et al., 2021). The typical subaerial characteristics of the upper units of SID indicate drier conditions compared to unit I, which can be related to the ongoing filling of the channel and lower moisture availability.

As the geomorphological setting is crucial not only for dust accumulation but also for preservation of LPSs especially (Lehmkuhl et al., 2016; Antoine et al., 2016; Marković et al., 2018), the favourable position of SID in a channel incised into an old Meuse River terrace led to a relatively thick accumulation of most likely Middle but especially Upper Pleniglacial sediments. Although LPSs in other extraordinary geomorphological situations such as loess dunes, so-called *gredas* (Antoine et al., 2001, 2009), or near watersheds (Henze, 1998; Zens et al., 2018) allow even thicker Pleniglacial loess deposits, the UPG record of SID exceeds those of many other regions in adjacent areas (Krauß et al., 2021; Antoine et al., 2016; Rahimzadeh et al., 2021; Krauß et al., 2016). Unit IV preserved 1 m of unaltered loess. Although loess formation generally continued throughout the late glacial in the Rhenish loess realm (Zens et al., 2018; Fischer et al., 2021), the SID sequence does not show any signs of late MIS 2 loess formation. The uppermost sample SID L2 within the Brabant loess yields quartz ages of 20.4 ± 1.5 ka (feldspar: 19.2 ± 1.1 ka), indicating late UPG ages for loess formation of the youngest preserved loess. Late glacial loess formation cannot be excluded for SID. However, these deposits were most likely eroded during the Pleistocene–Holocene transition. Extremely harsh and cold periglacial conditions during the UPG have influenced the sequence, as a large approx. 2 m deep ice-wedge pseudomorph pierced almost the entire sequence 3 m from the sampling spot (Fig. 2). As this cast is filled with material very similar to unit IV and pierces all underlying units, the age can be constrained to the UPG, although no direct timing was possible.

The LRE was strongly affected by anthropogenically induced soil erosion since the Early to Middle Holocene (Gerlach, 2006; Gerlach et al., 2006; Protze, 2014; Schulz, 2007; Gerz, 2017). However, the feldspar age calculated from the sample SID L1, taken from the base of the colluvial unit, yields a late glacial age (16.2 ± 0.8 ka). The quartz age (34.4 ± 2.5 ka) was excluded from the discussion, as it cannot be explained e.g. by partial bleaching possibly during

extreme precipitation events. As the widespread and intensive colluviation in the area only occurred in the Middle to Late Holocene (Schulz, 2007; Protze, 2014), it appears that the material was not fully bleached during relocation. Therefore, an exact timing of these erosional processes is not possible. Stratigraphical evidence of nearby exposures, however, indicates tectonic activities during the Late Pleistocene and Holocene, as features such as the decalcification boundary were affected by tectonic displacement. Therefore, the colluviation in SID could be the result of a landscape reorganisation due to tectonic movements in a highly active region (Fernández-Steeger et al., 2011; Reicherter et al., 2011; Grützner et al., 2016).

The sedimentary sequence of SID shows a complex interplay of various depositional milieus together with proposed active tectonic setting. It is a valuable archive for landscape dynamics in the LRE and suggests that the area was highly diverse during the Late Pleistocene. The high-resolution sedimentological, geochemical, and spectrophotometric analyses reveal a change from wetter conditions with ephemeral ponds and wetlands to a silting up of these wetlands and highly erosive conditions towards typical subaerial loess formation. The SID sequence, therefore, is a crucial addition to the framework of the landscape analyses of the Pleniglacial western ELB.

6 Conclusions

The Siersdorf LPS is an important site for Late Pleistocene dynamics of the Lower Rhine Embayment, indicating changing depositional environments during the period covered. The combination of sedimentological, geochemical, and spectrophotometric data with luminescence dating and tentative malacological tests shows that the sequence was under the influence of a marshy wetland environment during the late MPG and early UPGa, a unique feature for the LRE. Observed permafrost-induced conditions show the strong influence of the geomorphological setting and related processes on characteristics of sedimentary sequences. The UPGb was influenced by long-lasting erosional processes, which, however, were constrained to short-range transport mechanisms. The typical subaerial formation processes of the upper part of the sequence correlated to the UPGa, with typical regional marker horizons such as the Eben Zone, point to cold-arid conditions during this time, as observed for large parts of the European loess belt. Overall, this study stresses the importance of the geomorphological setting and related sedimentological and post-depositional processes in relation to the formation, preservation, and resulting characteristics of LPSs. Our results show not only that the LRE was subjected to fluctuating climate during the Pleniglacial but also that the area was more fragmented than previously thought, especially regarding the environmental setting.

Data availability. Data are available upon request to the corresponding author.

Supplement. The supplement related to this article is available online at: https://doi.org/10.5194/egqsj-72-77-2023-supplement.

Author contributions. SP designed the study together with FL and PS. PS, MK, FL, and SP took the analysed samples during two separate fieldwork campaigns in 2020. KS and DB performed luminescence dating and laboratory tests and compiled and discussed the results within the scientific framework. CR analysed the mollusc shells and fragments, which were provided by MK, and discussed their interpretability. SP wrote the initial draft of the manuscript with helpful comments and suggestions from the other authors. All authors discussed the data and participated in its interpretation.

Competing interests. The contact author has declared that none of the authors has any competing interests.

Disclaimer. Publisher's note: Copernicus Publications remains neutral with regard to jurisdictional claims in published maps and institutional affiliations.

Special issue statement. This article is part of the special issue "Quaternary research from and inspired by the first virtual DEUQUA conference". It is a result of the vDEUQUA2021 online conference in September/October 2021.

Acknowledgements. We thank Marianne Dohms, Renate Erdweg, and their team for the laboratory framework and Klaus Reicherter for his helpful comments on the tectonic evolution of the Lower Rhine Embayment in the field. We also thank the three anonymous reviewers for their constructive comments and remarks, which substantially improved this manuscript, and the editorial team for the uncomplicated handling of the manuscript.

Financial support. The investigations were carried out in the frame of the CRC 806 Our way to Europe – funded by the Deutsche Forschungsgemeinschaft (DFG, German Research Foundation, grant no. 57444011-SFB 806).

This open-access publication was funded by the RWTH Aachen University.

Review statement. This paper was edited by Julia Meister and reviewed by three anonymous referees.

References

Allen, J. R. L. and Thornley, D. M.: Laser granulometry of Holocene estuarine silts: effects of hydrogen peroxide treatment, Holocene, 14, 290–295, https://doi.org/10.1191/0959683604hl681rr, 2004.

Antoine, P., Rousseau, D.-D., Zöller, L., Lang, A., Munaut, A.-V., Hatté, C., and Fontugne, M.: High-resolution record of the last Interglacial–glacial cycle in the Nussloch loess–palaeosol sequences, Upper Rhine Area, Germany, Quatern. Int., 76–77, 211–229, https://doi.org/10.1016/S1040-6182(00)00104-X, 2001.

Antoine, P., Catt, J., Lautridou, J.-P., and Sommé, J.: The loess and coversands of northern France and southern England, J. Quaternary Sci., 18, 309–318, https://doi.org/10.1002/jqs.750, 2003.

Antoine, P., Rousseau, D.-D., Moine, O., Kunesch, S., Hatté, C., Lang, A., Tissoux, H., and Zöller, L.: Rapid and cyclic aeolian deposition during the Last Glacial in European loess: a high-resolution record from Nussloch, Germany, Quaternary Sci. Rev., 28, 2955–2973, https://doi.org/10.1016/j.quascirev.2009.08.001, 2009.

Antoine, P., Rousseau, D.-D., Degeai, J.-P., Moine, O., Lagroix, F., Kreutzer, S., Fuchs, M., Hatté, C., Gauthier, C., Svoboda, J., and Lisá, L.: High-resolution record of the environmental response to climatic variations during the Last Interglacial–Glacial cycle in Central Europe: the loess-palaeosol sequence of Dolní Věstonice (Czech Republic), Quaternary Sci. Rev., 67, 17–38, https://doi.org/10.1016/j.quascirev.2013.01.014, 2013.

Antoine, P., Goval, E., Jamet, G., Coutard, S., Moine, O., Hérisson, D., Auguste, P., Guérin, G., Lagroix, F., Schmidt, E., Robert, V., Debenham, N., Meszner, S., and Bahain, J.-J.: Les séquences loessiques pléistocène supérieur d'Havrincourt (Pas-de-Calais, France): stratigraphie, paléoenvironnements, géochronologie et occupations paléolithiques, Quaternaire, 25, 321–368, https://doi.org/10.4000/quaternaire.7278, 2014.

Antoine, P., Coutard, S., Guerin, G., Deschodt, L., Goval, E., Locht, J.-L., and Paris, C.: Upper Pleistocene loess-palaeosol records from Northern France in the European context: Environmental background and dating of the Middle Palaeolithic, Quatern. Int., 411, 4–24, https://doi.org/10.1016/j.quaint.2015.11.036, 2016.

Auclair, M., Lamothe, M., and Huot, S.: Measurement of anomalous fading for feldspar IRSL using SAR, Radiat. Meas., 37, 487–492, https://doi.org/10.1016/S1350-4487(03)00018-0, 2003.

Baykal, Y., Stevens, T., Engström-Johansson, A., Skurzyński, J., Zhang, H., He, J., Lu, H., Adamiec, G., Költringer, C., and Jary, Z.: Detrital zircon U–Pb age analysis of last glacial loess sources and proglacial sediment dynamics in the Northern European Plain, Quaternary Sci. Rev., 274, 107265, https://doi.org/10.1016/j.quascirev.2021.107265, 2021.

Boenigk, W. and Frechen, M.: The Pliocene and Quaternary fluvial archives of the Rhine system, Quaternary Sci. Rev., 25, 550–574, https://doi.org/10.1016/j.quascirev.2005.01.018, 2006.

Bokhorst, M. P., Vandenberghe, J., Sümegi, P., Łanczont, M., Gerasimenko, N. P., Matviishina, Z. N., Marković, S. B., and Frechen, M.: Atmospheric circulation patterns in central and eastern Europe during the Weichselian Pleniglacial inferred from loess grain-size records, Quatern. Int., 234, 62–74, https://doi.org/10.1016/j.quaint.2010.07.018, 2011.

Böse, M., Ehlers, J., and Lehmkuhl, F.: Der Mittelgebirgsrand, in: Deutschlands Norden, Springer, Berlin, Heidelberg, 63–87, https://doi.org/10.1007/978-3-662-64361-7_4, 2022.

Durcan, J. A., King, G., and Duller, G. A. T.: DRAC: Dose Rate and Age Calculator for trapped charge dating, Quat. Geochronol., 28, 54–61, https://doi.org/10.1016/j.quageo.2015.03.012, 2015.

Eckmeier, E. and Gerlach, R.: Characterization of Archaeological Soils and Sediments Using VIS Spectroscopy, eTopoi – Journal for Ancient Studies, 3, 285–290, https://doi.org/10.17169/refubium-21739, 2012.

Fenn, K., Durcan, J. A., Thomas, D. S. G., Millar, I. L., and Marković, S. B.: Re-analysis of late Quaternary dust mass accumulation rates in Serbia using new luminescence chronology for loess–palaeosol sequence at Surduk, Boreas, 49, 634–652, https://doi.org/10.1111/bor.12445, 2020.

Fenn, K., Thomas, D. S. G., Durcan, J. A., Millar, I. L., Veres, D., Piermattei, A., and Lane, C. S.: A tale of two signals: Global and local influences on the Late Pleistocene loess sequences in Bulgarian Lower Danube, Quaternary Sci. Rev., 274, 107264, https://doi.org/10.1016/j.quascirev.2021.107264, 2021.

Fernández-Steeger, T., Grützner, C., Reicherter, K., and Schaub, A.: Aquisgrani terrae motus factus est (part 1): The Aachen cathedral (Germany) built on weak ground?, Quatern. Int., 242, 138–148, https://doi.org/10.1016/j.quaint.2011.05.004, 2011.

Fischer, P., Hilgers, A., Protze, J., Kels, H., Lehmkuhl, F., and Gerlach, R.: Formation and geochronology of Last Interglacial to Lower Weichselian loess/palaeosol sequences – case studies from the Lower Rhine Embayment, Germany, E&G Quaternary Sci. J., 61, 48–63, https://doi.org/10.3285/eg.61.1.04, 2012.

Fischer, P., Hambach, U., Klasen, N., Schulte, P., Zeeden, C., Steininger, F., Lehmkuhl, F., Gerlach, R., and Radtke, U.: Landscape instability at the end of MIS 3 in western Central Europe: evidence from a multi proxy study on a Loess-Palaeosol-Sequence from the eastern Lower Rhine Embayment, Germany, Quatern. Int., 502, 119–136, https://doi.org/10.1016/j.quaint.2017.09.008, 2017.

Fischer, P., Jöris, O., Fitzsimmons, K. E., Vinnepand, M., Prud'homme, C., Schulte, P., Hatté, C., Hambach, U., Lindauer, S., Zeeden, C., Peric, Z., Lehmkuhl, F., Wunderlich, T., Wilken, D., Schirmer, W., and Vött, A.: Millennial-scale terrestrial ecosystem responses to Upper Pleistocene climatic changes: 4D-reconstruction of the Schwalbenberg Loess-Palaeosol-Sequence (Middle Rhine Valley, Germany), CATENA, 196, 104913, https://doi.org/10.1016/j.catena.2020.104913, 2021.

Frechen, M., Schweitzer, U., and Zander, A.: Improvements in sample preparation for the fine grain technique, Anc. TL, 14, 15–17, 1996.

Frechen, M., Oches, E. A., and Kohfeld, K. E.: Loess in Europe – mass accumulation rates during the Last Glacial Period, Quaternary Sci. Rev., 22, 1835–1857, https://doi.org/10.1016/S0277-3791(03)00183-5, 2003.

Gerlach, R.: Holozän: Die Umgestaltung der Landschaft durch den Menschen seit dem Neolithikum, in: Urgeschichte im Rheinland, edited by: Kunow, J. and Wegner, H., Verlag des Rheinischen Vereins für Denkmalpflege und Landschaftsschutz, Köln, 87–98, ISBN 9783880948143, 2006.

Gerlach, R., Baumewerd-Schmidt, H., van den Borg, K., Eckmeier, E., and Schmidt, M. W. I.: Prehistoric alteration of soil in the Lower Rhine Basin, Northwest Germany – archaeolog-

ical, 14C and geochemical evidence, Geoderma, 136, 38–50, https://doi.org/10.1016/j.geoderma.2006.01.011, 2006.

Gerz, J.: Prähistorische Mensch-Umwelt-Interaktionen im Spiegel von Kolluvien und Befundböden in zwei Löss-Altsiedellandschaften mit unterschiedlicher Boden- und Kulturgeschichte (Schwarzerderegion bei Halle/Saale und Parabraunerderegion Niederrheinische Bucht), Universitäts- und Stadtbibliothek Köln, Köln, URN urn:nbn:de:hbz:38-75297, 2017.

Grützner, C., Fischer, P., and Reicherter, K.: Holocene surface ruptures of the Rurrand Fault, Germany – insights from palaeoseismology, remote sensing and shallow geophysics, Geophys. J. Int., 204, 1662–1677, https://doi.org/10.1093/gji/ggv558, 2016.

Haesaerts, P., Juvigne, E., Kuyl, O., Mucher, H., and Roebroeks, W.: An account of the excursion of June, 13, 1981 in the Hesbaye area and to Dutch Limbourg, devoted to the chronostratigraphy of Upper Pleistocene loess, Ann.-Soc. Geol. Belg., 104, 223–240, 1981.

Haesaerts, P., Mestdagh, H., and Bosquet, D.: La séquence loessique de Remicourt (Hesbaye, Belgique), Notae Praehistoricae, 17, 45–52, 1997.

Haesaerts, P., Pirson, S., and Meijs, E.: Revised Lithostratigraphy of the aeolian loess deposits. Addendum to F. Gullentops et al. 2001. "Quaternary lithostratigraphic units (Belgium)", Geol. Belg., 4, 153–164, 2011.

Haesaerts, P., Damblon, F., Gerasimenko, N., Spagna, P., and Pirson, S.: The Late Pleistocene loess-palaeosol sequence of Middle Belgium, Quatern. Int., 411, 25–43, https://doi.org/10.1016/j.quaint.2016.02.012, 2016.

Hatté, C., Antoine, P., Fontugne, M., Lang, A., Rousseau, D.-D., and Zöller, L.: δ^{13}C of Loess Organic Matter as a Potential Proxy for Paleoprecipitation, Quaternary Res., 55, 33–38, https://doi.org/10.1006/qres.2000.2191, 2001.

Hatté, C., Gauthier, C., Rousseau, D.-D., Antoine, P., Fuchs, M., Lagroix, F., Marković, S. B., Moine, O., and Sima, A.: Excursions to C4 vegetation recorded in the Upper Pleistocene loess of Surduk (Northern Serbia): an organic isotope geochemistry study, Clim. Past, 9, 1001–1014, https://doi.org/10.5194/cp-9-1001-2013, 2013.

Henze, N.: Kennzeichnung des Oberwürmlösses der Niederrheinischen Bucht, Geologisches Institut der Universität zu Köln, Dissertation, Köln, 212 pp., ISBN 978-3-934027-00-8, 1998.

Hošek, J., Lisá, L., Hambach, U., Petr, L., Vejrostová, L., Bajer, A., Grygar, T. M., Moska, P., Gottvald, Z., and Horsák, M.: Middle Pleniglacial pedogenesis on the northwestern edge of the Carpathian basin: A multidisciplinary investigation of the Bíňa pedo-sedimentary section, SW Slovakia, Palaeogeogr. Palaeoclimatol. Palaeoecol., 487, 321–339, https://doi.org/10.1016/j.palaeo.2017.09.017, 2017.

ISO 20693: Soil quality – Determination of carbonate content – Volumetric method, International Organization for Standardization, Geneva, 1995.

Jary, Z.: Periglacial markers within the Late Pleistocene loess–palaeosol sequences in Poland and Western Ukraine, Quatern. Int., 198, 124–135, https://doi.org/10.1016/j.quaint.2008.01.008, 2009.

Jary, Z. and Ciszek, D.: Late Pleistocene loess–palaeosol sequences in Poland and western Ukraine, Quatern. Int., 296, 37–50, https://doi.org/10.1016/j.quaint.2012.07.009, 2013.

Kappler, C., Kaiser, K., Tanski, P., Klos, F., Fülling, A., Mrotzek, A., Sommer, M., and Bens, O.: Stratigraphy and age of colluvial deposits indicating Late Holocene soil erosion in northeastern Germany, CATENA, 170, 224–245, https://doi.org/10.1016/j.catena.2018.06.010, 2018.

Kels, H.: Bau und Bilanzierung der Lössdecke am westlichen Niederrhein, Heinrich-Heine-Universität Düsseldorf, URN urn:nbn:de:hbz:061-20070220-084835-4, 2007.

Klasen, N., Fischer, P., Lehmkuhl, F., and Hilgers, A.: Luminescence dating of loess deposits from the Remagen-Schwalbenberg site, Western Germany, Geochronometria, 42, https://doi.org/10.1515/geochr-2015-0008, 2015.

Klinge, M., Lehmkuhl, F., Schulte, P., Hülle, D., and Nottebaum, V.: Implications of (reworked) aeolian sediments and paleosols for Holocene environmental change in Western Mongolia, Geomorphology, 292, 59–71, https://doi.org/10.1016/j.geomorph.2017.04.027, 2017.

Knaak, M., Becker, S., Steffens, W., Mustereit, B., Hartkopf-Fröder, C., Prinz, L., Stichling, S., Schulte, P., and Lehmkuhl, F.: Boden des Jahres 2021 – ein Lössprofil auf der Aldenhovener Lössplatte, in: Archäologie im Rheinland 2020, Nünnerich-Asmus, Oppenheim, ISBN 978-3-96176-162-3, 2021.

Koch, R. and Neumeister, H.: Zur Klassifikation von Lösssedimenten nach genetischen Kriterien (About the classification of loess sediments using genetic criteria), Z. Geomorphol. NF, 49, 183–203, 2005.

Krauß, L., Zens, J., Zeeden, C., Schulte, P., Eckmeier, E., and Lehmkuhl, F.: A multi-proxy analysis of two loess-paleosol sequences in the northern Harz foreland, Germany, Palaeogeogr. Palaeoclimatol. Palaeoecol., 461, 401–417, https://doi.org/10.1016/j.palaeo.2016.09.001, 2016.

Krauß, L., Klasen, N., Schulte, P., and Lehmkuhl, F.: New results concerning the pedo- and chronostratigraphy of the loess–palaeosol sequence Attenfeld (Bavaria, Germany) derived from a multi-methodological approach, J. Quaternary Sci., 36, 1382–1396, https://doi.org/10.1002/jqs.3298, 2021.

Kühn, P., Lehndorff, E., and Fuchs, M.: Lateglacial to Holocene pedogenesis and formation of colluvial deposits in a loess landscape of Central Europe (Wetterau, Germany), CATENA, 154, 118–135, https://doi.org/10.1016/j.catena.2017.02.015, 2017.

Kukla, G., Heller, F., Ming, L. X., Chun, X. T., Sheng, L. T., and Sheng, A. Z.: Pleistocene climates in China dated by magnetic susceptibility, Geology, 16, 811–814, https://doi.org/10.1130/0091-7613(1988)016<0811:PCICDB>2.3.CO;2, 1988.

Lehmkuhl, F.: Modern and past periglacial features in Central Asia and their implication for paleoclimate reconstructions, Prog. Phys. Geogr. Earth Environ., 40, 369–391, https://doi.org/10.1177/0309133315615778, 2016.

Lehmkuhl, F., Wirtz, S., Falk, D., and Kels, H.: Geowissenschaftliche Untersuchungen zur Landschaftsentwicklung im Tagebau Garzweiler – LANU-Projekt 2012–2014, in: Archäologie im Rheinland 2014, edited by: Kunow, J. and Trier, M., Theiss Verlag, Stuttgart, 64–66, ISBN 978-3-8062-3214-1, 2015.

Lehmkuhl, F., Zens, J., Krauß, L., Schulte, P., and Kels, H.: Loess-paleosol sequences at the northern European loess belt in Germany: Distribution, geomorphology and stratigraphy, Quaternary Sci. Rev., 153, 11–30, https://doi.org/10.1016/j.quascirev.2016.10.008, 2016.

Lehmkuhl, F., Pötter, S., Pauligk, A., and Bösken, J.: Loess and other Quaternary sediments in Germany, J. Maps, 14, 330–340, https://doi.org/10.1080/17445647.2018.1473817, 2018.

Lehmkuhl, F., Nett, J. J., Pötter, S., Schulte, P., Sprafke, T., Jary, Z., Antoine, P., Wacha, L., Wolf, D., Zerboni, A., Hošek, J., Marković, S. B., Obreht, I., Sümegi, P., Veres, D., Zeeden, C., Boemke, B. J., Schaubert, V., Viehweger, J., and Hambach, U.: Loess landscapes of Europe – mapping, geomorphology, and zonal differentiation, Earth-Sci. Rev., 215, 103496, https://doi.org/10.1016/j.earscirev.2020.103496, 2021.

Marković, S. B., McCoy, W. D., Oches, E. A., Savic, S., Gaudenyi, T., Jovanovic, M., Stevens, T., Walther, R., Ivanisevic, P., and Galic, Z.: Paleoclimate record in the Upper Pleistocene loess-paleosol sequence at Petrovaradin brickyard (Vojvodina, Serbia), Geol. Carpathica, 56, 545–552, 2005.

Marković, S. B., Stevens, T., Kukla, G. J., Hambach, U., Fitzsimmons, K. E., Gibbard, P., Buggle, B., Zech, M., Guo, Z., Hao, Q., Wu, H., O'Hara Dhand, K., Smalley, I. J., Újvári, G., Sümegi, P., Timar-Gabor, A., Veres, D., Sirocko, F., Vasiljević, D. A., Jary, Z., Svensson, A., Jović, V., Lehmkuhl, F., Kovács, J., and Svirčev, Z.: Danube loess stratigraphy – Towards a pan-European loess stratigraphic model, Earth-Sci. Rev., 148, 228–258, https://doi.org/10.1016/j.earscirev.2015.06.005, 2015.

Marković, S. B., Stevens, T., Mason, J., Vandenberghe, J., Yang, S., Veres, D., Újvári, G., Timar-Gabor, A., Zeeden, C., Guo, Z., Hao, Q., Obreht, I., Hambach, U., Wu, H., Gavrilov, M. B., Rolf, C., Tomić, N., and Lehmkuhl, F.: Loess correlations – Between myth and reality, Palaeogeogr. Palaeoclimatol. Palaeoecol., 509, 4–23, https://doi.org/10.1016/j.palaeo.2018.04.018, 2018.

Mayr, C., Matzke-Karasz, R., Stojakowits, P., Lowick, S. E., Zolitschka, B., Heigl, T., Mollath, R., Theuerkauf, M., Weckend, M.-O., Bäumler, R., and Gregor, H.-J.: Palaeoenvironments during MIS 3 and MIS 2 inferred from lacustrine intercalations in the loess–palaeosol sequence at Bobingen (southern Germany), E&G Quaternary Sci. J., 66, 73–89, https://doi.org/10.5194/egqsj-66-73-2017, 2017.

Meijs, E. P. M.: Loess stratigraphy in Dutch and Belgian Limburg, E&G Quaternary Sci. J., 51, 115–131, https://doi.org/10.3285/eg.51.1.08, 2002.

Meszner, S., Fuchs, M., and Faust, D.: Loess-Palaeosol-Sequences from the loess area of Saxony (Germany), E&G Quaternary Sci. J., 60, 4, https://doi.org/10.3285/eg.60.1.03, 2011.

Meszner, S., Kreutzer, S., Fuchs, M., and Faust, D.: Late Pleistocene landscape dynamics in Saxony, Germany: Paleoenvironmental reconstruction using loess-paleosol sequences, Quatern. Int., 296, 94–107, https://doi.org/10.1016/j.quaint.2012.12.040, 2013.

Meszner, S., Kreutzer, S., Fuchs, M., and Faust, D.: Identifying depositional and pedogenetic controls of Late Pleistocene loess-paleosol sequences (Saxony, Germany) by combined grain size and microscopic analyses, Z. Geomorphol., 58, 63–90, https://doi.org/10.1127/0372-8854/2014/S-00169, 2014.

Meyer-Heintze, S., Sprafke, T., Schulte, P., Terhorst, B., Lomax, J., Fuchs, M., Lehmkuhl, F., Neugebauer-Maresch, C., Einwögerer, T., Händel, M., Simon, U., and Solís Castillo, B.: The MIS 3/2 transition in a new loess profile at Krems-Wachtberg East – A multi-methodological approach, Quatern. Int., 464, 370–385, https://doi.org/10.1016/j.quaint.2017.11.048, 2018.

Moine, O.: West-european malacofauna from loess deposits of the weichselian upper pleniglacial: Compilation and preliminary analysis of the database, Quaternaire, 19, 11–29, https://doi.org/10.4000/quaternaire.1532, 2008.

Murray, A. S. and Wintle, A. G.: Luminescence dating of quartz using an improved single-aliquot regenerative-dose protocol, Radiat. Meas., 32, 57–73, https://doi.org/10.1016/S1350-4487(99)00253-X, 2000.

Nesbitt, H. W. and Young, G. M.: Early Proterozoic climates and plate motions inferred from major element chemistry of lutites, Nature, 299, 715–717, https://doi.org/10.1038/299715a0, 1982.

Nesbitt, H. W. and Young, G. M.: Prediction of some weathering trends of plutonic and volcanic rocks based on thermodynamic and kinetic considerations, Geochim. Cosmochim. Ac., 48, 1523–1534, https://doi.org/10.1016/0016-7037(84)90408-3, 1984.

Nottebaum, V., Stauch, G., Hartmann, K., Zhang, J., and Lehmkuhl, F.: Unmixed loess grain size populations along the northern Qilian Shan (China): Relationships between geomorphologic, sedimentologic and climatic controls, Quatern. Int., 372, 151–166, https://doi.org/10.1016/j.quaint.2014.12.071, 2015.

Obreht, I., Zeeden, C., Schulte, P., Hambach, U., Eckmeier, E., Timar-Gabor, A., and Lehmkuhl, F.: Aeolian dynamics at the Orlovat loess–paleosol sequence, northern Serbia, based on detailed textural and geochemical evidence, Aeolian Res., 18, 69–81, https://doi.org/10.1016/j.aeolia.2015.06.004, 2015.

Obreht, I., Hambach, U., Veres, D., Zeeden, C., Bösken, J., Stevens, T., Marković, S. B., Klasen, N., Brill, D., Burow, C., and Lehmkuhl, F.: Shift of large-scale atmospheric systems over Europe during late MIS 3 and implications for Modern Human dispersal, Sci. Rep., 7, 5848, https://doi.org/10.1038/s41598-017-06285-x, 2017.

Ohta, T.: Geochemistry of Jurassic to earliest Cretaceous deposits in the Nagato Basin, SW Japan: implication of factor analysis to sorting effects and provenance signatures, Sediment. Geol., 171, 159–180, https://doi.org/10.1016/j.sedgeo.2004.05.014, 2004.

Özer, M., Orhan, M., and Işik, N. S.: Effect of particle optical properties on size distribution of soils obtained by laser diffraction, Environ. Eng. Geosci., 16, 163–173, 2010.

Pécsi, M.: Loess is not just the accumulation of dust, Quatern. Int., 7–8, 1–21, https://doi.org/10.1016/1040-6182(90)90034-2, 1990.

Pécsi, M. and Richter, G.: Löß: Herkunft – Gliederung – Landschaften, Borntraeger, Berlin, 391 pp., ISBN 978-3-443-21098-4, 1996.

Pötter, S., Veres, D., Baykal, Y., Nett, J. J., Schulte, P., Hambach, U., and Lehmkuhl, F.: Disentangling sedimentary pathways for the Pleniglacial Lower Danube loess based on geochemical signatures, Front. Earth Sci., 9, 1–25, https://doi.org/10.3389/feart.2021.600010, 2021.

Protze, J.: Eine "Mensch gemachte Landschaft" – Diachrone, geochemische und sedimentologische Untersuchungen an anthropogen beeinflussten Sedimenten und Böden der Niederrheinischen Lössbörde, Hochschulbibliothek der Rheinisch-Westfälischen Technischen Hochschule Aachen, Aachen, URN urn:nbn:de:hbz:82-opus-49066, 2014.

Rahimzadeh, N., Sprafke, T., Thiel, C., Terhorst, B., and Frechen, M.: A comparison of polymineral and K-feldspar post-infrared infrared stimulated luminescence ages of loess from Franco-

nia, southern Germany, E&G Quaternary Sci. J., 70, 53–71, https://doi.org/10.5194/egqsj-70-53-2021, 2021.

Reicherter, K., Schaub, A., Fernández-Steeger, T., Grützner, C., and Kohlberger-Schaub, T.: Aquisgrani terrae motus factus est (part 2): Evidence for medieval earthquake damage in the Aachen Cathedral (Germany), Quatern. Int., 242, 149–157, https://doi.org/10.1016/j.quaint.2011.05.006, 2011.

Rousseau, D.-D. and Hatté, C.: Ground-Air Interface: The Loess Sequences, Markers of Atmospheric Circulation, in: Paleoclimatology, edited by: Ramstein, G., Landais, A., Bouttes, N., Sepulchre, P., and Govin, A., Springer International Publishing, Cham, 157–167, https://doi.org/10.1007/978-3-030-24982-3_13, 2021.

Rousseau, D.-D., Antoine, P., and Sun, Y.: How dusty was the last glacial maximum over Europe?, Quaternary Sci. Rev., 254, 106775, https://doi.org/10.1016/j.quascirev.2020.106775, 2021.

Schaller, K.: Praktikum Zur Bodenkunde Und Pflanzenernährung, 8th edn., Forschungsanstalt Geisenheim, Geisenheim, ISBN 978-3980187213, 2000.

Schirmer, W.: Eine Klimakurve des Oberpleistozäns aus dem rheinischen Löss, E&G Quaternary Sci. J., 50, 25–49, https://doi.org/10.3285/eg.50.1.02, 2000.

Schirmer, W.: Compendium of the Rhein loess sequence, Terra Nostra, 10, 8–23, 2002.

Schirmer, W.: Die Eben-Zone im Oberwürmlöss zwischen Maas und Rhein, in: Landschaftsgeschichte im Europäischen Rheinland, vol. 4, edited by: Schirmer, W., LIT Verlag, Münster, 351–416, ISBN 978-3-825-86009-7, 2003.

Schirmer, W.: Late Pleistocene loess of the Lower Rhine, Quatern. Int., 411, 44–61, https://doi.org/10.1016/j.quaint.2016.01.034, 2016.

Schirmer, W., Ikinger, A., and Nehring, F.: Die terrestrischen Böden im Profil Schwalbenberg/Mittelrhein (Terrestrial soils of the Schwalbenberg profile/Middle Rhine), Mainzer Geowissenschaftliche Mitteilungen, 40, 53–78, 2012.

Schulte, P. and Lehmkuhl, F.: The difference of two laser diffraction patterns as an indicator for post-depositional grain size reduction in loess-paleosol sequences, Palaeogeogr. Palaeoclimatol. Palaeoecol., 509, 126–136, https://doi.org/10.1016/j.palaeo.2017.02.022, 2018.

Schulte, P., Lehmkuhl, F., Steininger, F., Loibl, D., Lockot, G., Protze, J., Fischer, P., and Stauch, G.: Influence of HCl pretreatment and organo-mineral complexes on laser diffraction measurement of loess–paleosol-sequences, CATENA, 137, 392–405, https://doi.org/10.1016/j.catena.2015.10.015, 2016.

Schulz, W.: Die Kolluvien der westlichen Kölner Bucht – Gliederung, Entstehungszeit und geomorphologische Bedeutung, Universitäts- und Stadtbibliothek Köln, Cologne, Germany, URN urn:nbn:de:hbz:38-19656, 2007.

Sedov, S., Rusakov, A., Sheinkman, V., and Korkka, M.: MIS3 paleosols in the center-north of Eastern Europe and Western Siberia: Reductomorphic pedogenesis conditioned by permafrost?, CATENA, 146, 38–47, https://doi.org/10.1016/j.catena.2016.03.022, 2016.

Sirocko, F., Knapp, H., Dreher, F., Förster, M. W., Albert, J., Brunck, H., Veres, D., Dietrich, S., Zech, M., Hambach, U., Röhner, M., Rudert, S., Schwibus, K., Adams, C., and Sigl, P.: The ELSA-Vegetation-Stack: Reconstruction of Landscape Evolution Zones (LEZ) from laminated Eifel maar sediments of the last 60 000 years, Glob. Planet. Change, 142, 108–135, https://doi.org/10.1016/j.gloplacha.2016.03.005, 2016.

Skurzyński, J., Jary, Z., Raczyk, J., Moska, P., Korabiewski, B., Ryzner, K., and Krawczyk, M.: Geochemical characterization of the Late Pleistocene loess-palaeosol sequence in Tyszowce (Sokal Plateau-Ridge, SE Poland), Quatern. Int., 502, 108–118, https://doi.org/10.1016/j.quaint.2018.04.023, 2019.

Skurzyński, J., Jary, Z., Kenis, P., Kubik, R., Moska, P., Raczyk, J., and Seul, C.: Geochemistry and mineralogy of the Late Pleistocene loess-palaeosol sequence in Złota (near Sandomierz, Poland): Implications for weathering, sedimentary recycling and provenance, Geoderma, 375, 114459, https://doi.org/10.1016/j.geoderma.2020.114459, 2020.

Sprafke, T. and Obreht, I.: Loess: Rock, sediment or soil – What is missing for its definition?, Quatern. Int., 399, 198–207, https://doi.org/10.1016/j.quaint.2015.03.033, 2016.

Stadelmaier, K. H., Ludwig, P., Bertran, P., Antoine, P., Shi, X., Lohmann, G., and Pinto, J. G.: A new perspective on permafrost boundaries in France during the Last Glacial Maximum, Clim. Past, 17, 2559–2576, https://doi.org/10.5194/cp-17-2559-2021, 2021.

Steup, R. and Fuchs, M.: The loess sequence at Münzenberg (Wetterau/Germany): A reinterpretation based on new luminescence dating results, Z. Geomorphol., 61, 101–120, https://doi.org/10.1127/zfg_suppl/2016/0408, 2017.

Stevens, T., Sechi, D., Bradák, B., Orbe, R., Baykal, Y., Cossu, G., Tziavaras, C., Andreucci, S., and Pascucci, V.: Abrupt last glacial dust fall over southeast England associated with dynamics of the British-Irish ice sheet, Quaternary Sci. Rev., 250, 106641, https://doi.org/10.1016/j.quascirev.2020.106641, 2020.

Sümegi, P., Náfrádi, K., Molnár, D., and Sávai, S.: Results of paleoecological studies in the loess region of Szeged-Öthalom (SE Hungary), Quatern. Int., 372, 66–78, https://doi.org/10.1016/j.quaint.2014.09.003, 2015.

Svirčev, Z., Marković, S. B., Stevens, T., Codd, G. A., Smalley, I., Simeunović, J., Obreht, I., Dulić, T., Pantelić, D., and Hambach, U.: Importance of biological loess crusts for loess formation in semi-arid environments, Quatern. Int., 296, 206–215, https://doi.org/10.1016/j.quaint.2012.10.048, 2013.

Thiel, C., Buylaert, J.-P., Murray, A., Terhorst, B., Hofer, I., Tsukamoto, S., and Frechen, M.: Luminescence dating of the Stratzing loess profile (Austria) – Testing the potential of an elevated temperature post-IR IRSL protocol, Quatern. Int., 234, 23–31, https://doi.org/10.1016/j.quaint.2010.05.018, 2011.

Torre, G., Gaiero, D. M., Cosentino, N. J., and Coppo, R.: The paleoclimatic message from the polymodal grain-size distribution of late Pleistocene-early Holocene Pampean loess (Argentina), Aeolian Res., 42, 100563, https://doi.org/10.1016/j.aeolia.2019.100563, 2020.

Vandenberghe, J., French, H. M., Gorbunov, A., Marchenko, S., Velichko, A. A., Jin, H., Cui, Z., Zhang, T., and Wan, X.: The Last Permafrost Maximum (LPM) map of the Northern Hemisphere: permafrost extent and mean annual air temperatures, 25–17 ka BP: The Last Permafrost Maximum (LPM) map of the Northern Hemisphere, Boreas, 43, 652–666, https://doi.org/10.1111/bor.12070, 2014.

Varga, A., Újvári, G., and Raucsik, B.: Tectonic versus climatic control on the evolution of a loess–paleosol sequence at Beremend, Hungary: an integrated approach based on paleoecological, clay

mineralogical, and geochemical data, Quatern. Int., 240, 71–86, https://doi.org/10.1016/j.quaint.2010.10.032, 2011.

Veres, D., Tecsa, V., Gerasimenko, N., Zeeden, C., Hambach, U., and Timar-Gabor, A.: Short-term soil formation events in last glacial east European loess, evidence from multi-method luminescence dating, Quaternary Sci. Rev., 200, 34–51, https://doi.org/10.1016/j.quascirev.2018.09.037, 2018.

Vinnepand, M., Fischer, P., Fitzsimmons, K., Thornton, B., Fiedler, S., and Vött, A.: Combining Inorganic and Organic Carbon Stable Isotope Signatures in the Schwalbenberg Loess-Palaeosol-Sequence Near Remagen (Middle Rhine Valley, Germany), Front. Earth Sci., 8, 276, https://doi.org/10.3389/feart.2020.00276, 2020.

Vinnepand, M., Fischer, P., Jöris, O., Hambach, U., Zeeden, C., Schulte, P., Fitzsimmons, K. E., Prud'homme, C., Perić, Z., Schirmer, W., Lehmkuhl, F., Fiedler, S., and Vött, A.: Decoding geochemical signals of the Schwalbenberg Loess-Palaeosol-Sequences – A key to Upper Pleistocene ecosystem responses to climate changes in western Central Europe, CATENA, 212, 106076, https://doi.org/10.1016/j.catena.2022.106076, 2022.

Vlaminck, S., Kehl, M., Lauer, T., Shahriari, A., Sharifi, J., Eckmeier, E., Lehndorff, E., Khormali, F., and Frechen, M.: Loess-soil sequence at Toshan (Northern Iran): Insights into late Pleistocene climate change, Quatern. Int., 399, 122–135, https://doi.org/10.1016/j.quaint.2015.04.028, 2016.

Zech, M., Zech, R., Buggle, B., and Zöller, L.: Novel methodological approaches in loess research – interrogating biomarkers and compound-specific stable isotopes, E&G Quaternary Sci. J., 60, 13, https://doi.org/10.3285/eg.60.1.12, 2011.

Zech, R., Zech, M., Marković, S., Hambach, U., and Huang, Y.: Humid glacials, arid interglacials? Critical thoughts on pedogenesis and paleoclimate based on multi-proxy analyses of the loess–paleosol sequence Crvenka, Northern Serbia, Palaeogeogr. Palaeoclimatol. Palaeoecol., 387, 165–175, https://doi.org/10.1016/j.palaeo.2013.07.023, 2013.

Zens, J., Zeeden, C., Römer, W., Fuchs, M., Klasen, N., and Lehmkuhl, F.: The Eltville Tephra (Western Europe) age revised: Integrating stratigraphic and dating information from different Last Glacial loess localities, Palaeogeogr. Palaeoclimatol. Palaeoecol., 466, 240–251, https://doi.org/10.1016/j.palaeo.2016.11.033, 2017.

Zens, J., Schulte, P., Klasen, N., Krauß, L., Pirson, S., Burow, C., Brill, D., Eckmeier, E., Kels, H., Zeeden, C., Spagna, P., and Lehmkuhl, F.: OSL chronologies of paleoenvironmental dynamics recorded by loess-paleosol sequences from Europe: Case studies from the Rhine-Meuse area and the Neckar Basin, Palaeogeogr. Palaeoclimatol. Palaeoecol., 509, 105–125, https://doi.org/10.1016/j.palaeo.2017.07.019, 2018.